Dielectric relaxation of chained ferrofluids

Dielectric relaxation of chained ferrofluids

Vladimir V. Murashov, Philip J. Camp, and G. N. Patey

Citation: J. Chem. Phys. **116**, 6731 (2002); doi: 10.1063/1.1462042
View online: http://dx.doi.org/10.1063/1.1462042
View Table of Contents: http://jcp.aip.org/resource/1/JCPSA6/v116/i15
Published by the AIP Publishing LLC.

Dielectric relaxation of chained ferrofluids

Vladimir V. Murashov
Department of Chemistry, University of British Columbia, Vancouver, British Columbia, Canada, V6T 1Z1

Philip J. Camp
Department of Chemistry, University of Edinburgh, West Mains Road, Edinburgh EH9 3JJ, United Kingdom

G. N. Patey
Department of Chemistry, University of British Columbia, Vancouver, British Columbia, Canada, V6T 1Z1

(Received 2 October 2001; accepted 25 January 2002)

Molecular and Brownian dynamics simulations are used to investigate the frequency-dependent dielectric relaxation of ferrofluids, with the objective of identifying features characteristic of dipolar chain formation at low densities. It is shown that the presence of chains gives rise to a high frequency band associated with the vibrational motion of dipoles within the chains. This band serves as a ''signature'' of association and is not present in dipolar fluids at higher, liquid-like densities. A simple theory that traps the basic features of the relaxation behavior is also presented. © *2002 American Institute of Physics.* [DOI: 10.1063/1.1462042]

I. INTRODUCTION

In recent years there has been considerable interest in the structure and phase behavior of strongly interacting dipolar fluids.[1,2] Computer simulations have shown[3,4] that such systems exhibit at least three fluid phases: a high density ferroelectric liquid, and two orientationally disordered phases at low and intermediate densities. The disordered ''liquid'' phase behaves in an essentially ''normal'' manner, but in the low temperature ''gas'' phase the particles assemble to form extensive chain-like structures. The unusual phase behavior of these systems has also been the subject of an interesting theoretical analysis.[1] Furthermore, similar chain-like structures were observed experimentally in colloidal ferrofluids thirty-five years ago.[5]

The present paper was partially motivated by recent work of Mamiya *et al.*[6] These authors attempted to detect phase transitions in colloidal ferrofluids by measuring magnetic susceptibilities. They report evidence of a first-order phase transition that appears to be related to the condensation observed in computer simulations. Here, we employ both molecular dynamics (MD) and Brownian dynamics (BD) simulations in order to investigate the dielectric relaxation of dipolar fluids at low temperatures and densities (note that this is analogous to magnetic relaxation in ferrofluids). We observe and discuss relaxations associated with the motion of chains and of dipoles within chains. This should provide a guide for the identification of chained or associated states by means of relaxation experiments.

II. THE MODEL AND SIMULATION METHODS

We consider fluids of dipolar soft spheres of mass m, moment of inertia I, and interacting via the pair potential

$$u(12)=4\varepsilon(\sigma/r)^{12}-3(\boldsymbol{\mu}_1\cdot\mathbf{r})(\boldsymbol{\mu}_2\cdot\mathbf{r})/r^5+\boldsymbol{\mu}_1\cdot\boldsymbol{\mu}_2/r^3, \qquad (1)$$

where ε and σ characterize the soft-sphere interaction, $\boldsymbol{\mu}_i$ is the dipole associated with particle i, $\mathbf{r}$ is the interparticle vector and $r=|\mathbf{r}|$. In order to characterize the systems considered, it is convenient to introduce the following reduced parameters: density, $\rho^*=N\sigma^3/V$, where N is the number of particles and V is the volume of the system; temperature, $T^*=kT/\varepsilon$, where k is the Boltzmann constant; dipole moment, $\mu^*=\mu/(\varepsilon\sigma^3)^{1/2}$; moment of inertia, $I^*=I/(m\sigma^2)$; time, $t^*=t(\varepsilon/m\sigma^2)^{1/2}$; and angular velocity, $\omega^*=\omega(\varepsilon/m\sigma^2)^{-1/2}$. Additionally, the BD calculations require the reduced translational and rotational diffusion constants, denoted by $D^*=D(\varepsilon\sigma^2/m)^{-1/2}$ and $\Theta^*=\Theta(\varepsilon/m\sigma^2)^{-1/2}$, respectively.

Simulations were performed using standard MD[7] and BD techniques.[7–9] While we would not expect either of these methods to correspond exactly to the situation in a colloidal ferrofluid, the fact that both yield qualitatively similar results gives us confidence that the behavior we observe is physically meaningful. In all calculations cubic cells with periodic boundary conditions were employed, and the long-range forces were handled using the Ewald summation method with conducting boundary conditions.[10] The equations-of-motion were integrated using a fifth-order Gear predictor–corrector algorithm with a time step $\Delta t^*=0.002$. All results reported were obtained with 256 particles.

III. A SIMPLE THEORY OF DIELECTRIC RELAXATION AT LOW TEMPERATURE AND DENSITY

Before discussing the simulation results, it is instructive to consider the dielectric behavior one might expect to observe in systems with a high degree of dipolar association.

Consider a chain of dipolar particles separated by a typical ''hard-core'' diameter, σ. For each dipole there will be a strong preference to align along the chain, due largely to the influence of other dipoles in the vicinity. We can approximate the local mean field experienced by a particular dipole as that due to an infinite linear chain of dipoles (each with the mean orientation) extending in either direction.[11] The mean dipolar orientation is given by $\langle\cos\gamma\rangle$, where γ is the

polar angle between a dipole and the local chain direction, and $\langle \cdots \rangle$ denotes a Boltzmann-weighted average. The mean-field interaction energy, u_{MF}, between a given dipole and the remainder of the chain can therefore be estimated by

$$u_{\mathrm{MF}} = -\sum_{n=1}^{\infty} \frac{4\mu^2 \langle \cos\gamma \rangle \cos\gamma}{(n\sigma)^3} = -\frac{4\zeta(3)\mu^2 \langle \cos\gamma \rangle \cos\gamma}{\sigma^3}, \tag{2}$$

where $\zeta(x)$ is the Riemann zeta function. The self-consistent mean-field equation for $\langle \cos\gamma \rangle$ is,

$$\langle \cos\gamma \rangle = \frac{\int_{-1}^{1} \cos\gamma e^{4\lambda \langle \cos\gamma \rangle \cos\gamma} \mathrm{d}\cos\gamma}{\int_{-1}^{1} e^{4\lambda \langle \cos\gamma \rangle \cos\gamma} \mathrm{d}\cos\gamma} = \coth(4\lambda\langle\cos\gamma\rangle) - \frac{1}{4\lambda\langle\cos\gamma\rangle}, \tag{3}$$

where $\lambda = \zeta(3)\mu^2/k_{\mathrm{B}}T\sigma^3$ is a dimensionless interaction parameter. Equation (3) is a transcendental equation which can be solved for $\langle \cos\gamma \rangle$. For $\lambda < 3/4$ the solution of the self-consistent mean-field relation (3) is $\langle \cos\gamma \rangle = 0$, i.e., the distribution of dipole orientations in the chain is isotropic. For $\lambda > 3/4$, however, $0 < \langle \cos\gamma \rangle \leqslant 1$, corresponding to the alignment of the dipoles along the chain. At low temperature and density the typical deviation from perfect alignment of a dipole will be small, i.e., $\cos\gamma \approx 1 - \frac{1}{2}\gamma^2$. In the limit $\lambda^{-1} \to 0$, Eq. (3) can be solved analytically:

$$\langle \cos\gamma \rangle \approx \tfrac{1}{2} + \tfrac{1}{2}\sqrt{1-\lambda^{-1}}, \tag{4}$$

$$\langle \gamma^2 \rangle \approx 1 - \sqrt{1-\lambda^{-1}}. \tag{5}$$

This specifies our approximation for the mean-field interactions within the chains.

We construct a simple mean-field theory for the dielectric relaxation in the following way. First, we examine the dynamics of a single dipole in the mean field of the other dipoles in the chain, taking into account the rotation of the chain as a whole, but assuming no friction. Next, we add exponential factors with characteristic relaxation times to take account of the rotational and vibrational friction. Last, we invoke the "corresponding micro–macro correlation" theorem (CMMC)[12,13] to relate the single-particle correlation function to the macroscopic correlation function.

It is convenient to consider a dipole unit vector oscillating in the (y,z) plane of a local frame such that,

$$\mu_x^l(t) = 0, \quad \mu_y^l(t) = -\sin\gamma(t), \quad \mu_z^l(t) = \cos\gamma(t), \tag{6}$$

where the superscript "l" denotes the local frame. The resultant torque on the dipole due to the mean field is therefore,

$$\dot{\mathbf{L}} = -\frac{4\zeta(3)\mu^2 \langle \cos\gamma \rangle \sin\gamma}{\sigma^3} \hat{\mathbf{e}}_x^l, \tag{7}$$

where $\mathbf{L} = I\dot{\gamma}\hat{\mathbf{e}}_x^l$ is the angular momentum, and $\hat{\mathbf{e}}_x^l$ is a unit vector along the local x-axis. As above, we study the low-temperature regime in which the oscillations of the dipole are small, and so $\sin\gamma \approx \gamma$. Solving the equation of motion, $\dot{L} = I\ddot{\gamma}$, with this approximation gives for $\gamma(t)$,

$$\gamma(t) = \gamma(0)\cos\omega_0 t + \omega_0^{-1}\dot{\gamma}(0)\sin\omega_0 t, \tag{8}$$

where $\omega_0 = \sqrt{4\zeta(3)\mu^2\langle\cos\gamma\rangle/I\sigma^3}$ is the angular frequency of the oscillation. This specifies the dynamics of the dipole in the local frame, assuming no friction.

We now consider the dynamics in the chain-fixed frame. If the local dipole frame is specified by the Euler angles (ϕ,θ,ψ),[14] then the components of the unit dipole vector in a chain-fixed frame are given by,

$$\begin{aligned} \mu_x^c(t) &= [(\cos\phi\sin\psi + \sin\phi\cos\theta\cos\psi)\sin\gamma(t) \\ &\quad + \sin\phi\sin\theta\cos\gamma(t)], \\ \mu_y^c(t) &= [(\sin\phi\sin\psi - \cos\phi\cos\theta\cos\psi)\sin\gamma(t) \\ &\quad - \cos\phi\sin\theta\cos\gamma(t)], \\ \mu_z^c(t) &= [-\sin\theta\cos\psi\sin\gamma(t) + \cos\theta\cos\gamma(t)], \end{aligned} \tag{9}$$

where the superscript "c" denotes the chain-fixed frame.

In the laboratory frame, the chain rotates about the x-axis with a typical frequency, Ω_0. Hence, the components of the unit dipole vector in the laboratory frame are given by

$$\begin{aligned} \mu_x(t) &= \mu_x^c(t), \\ \mu_y(t) &= \mu_y^c(t)\cos\Omega_0 t - \mu_z^c(t)\sin\Omega_0 t, \\ \mu_z(t) &= \mu_y^c(t)\sin\Omega_0 t + \mu_z^c(t)\cos\Omega_0 t. \end{aligned} \tag{10}$$

We next assume that the chains in question are long and twisted (see Figs. 2 and 3) such that the system has no net orientational order. Under this assumption, the single-particle correlation function, $\Phi_S(t)$, is given by

$$\Phi_S(t) = \frac{1}{8\pi^2}\int_0^{2\pi}\mathrm{d}\phi\int_{-1}^{1}\mathrm{d}\cos\theta\int_0^{2\pi}\mathrm{d}\psi\langle\hat{\mu}(t)\cdot\hat{\mu}(0)\rangle, \tag{11}$$

where $\langle \cdots \rangle$ denotes an ensemble average over initial local angles, $\gamma(0)$, and initial angular velocities, $\dot{\gamma}(0)$. Inserting Eqs. (9) and (10) into Eq. (11), and performing the integrations over the Euler angles (ϕ,θ,ψ), we obtain,

$$\Phi_S(t) = \frac{1+2\cos\Omega_0 t}{3}[\langle\sin\gamma(t)\sin\gamma(0) + \cos\gamma(t)\cos\gamma(0)\rangle]. \tag{12}$$

For small oscillations, the equation-of-motion for $\gamma(t)$ [Eq. (8)] can be inserted into Eq. (12) to yield,

$$\Phi_S(t) \approx \frac{1+2\cos\Omega_0 t}{3}[1-\langle\gamma^2\rangle+\langle\gamma(t)\gamma(0)\rangle]$$

$$=\frac{1+2\cos\Omega_0 t}{3}[1-\langle\gamma^2\rangle+\langle\gamma^2\rangle\cos\omega_0 t]. \quad (13)$$

The $\omega_0^{-1}\dot{\gamma}(t)\sin\omega_0 t$ term in Eq. (8) disappears since $\langle\dot{\gamma}(t)\rangle=0$.

In the previous discussion, we have completely ignored the influence of friction. At this point, we assume that both the rotational and vibrational contributions to the correlation function decay exponentially and are characterized by different relaxation times, τ_R and τ_V, respectively. We emphasize that this is to some extent just an "educated guess," but we see below (see Sec. IV) that it corresponds quite closely to the actual simulation results. With this assumption, the self-correlation function takes the form

$$\Phi_S(t)=\frac{1+2\cos\Omega_0 t}{3}\exp(-t/\tau_R)$$

$$\times[1-\langle\gamma^2\rangle+\langle\gamma^2\rangle\cos(\omega_0 t)\exp(-t/\tau_V)]. \quad (14)$$

The CMMC theorem[12,13] states that if the molecular correlation function, $\Phi_S(t)$, can be expressed as a sum of exponentials, then the macroscopic correlation function, $\Phi_M(t)$, has the same form but with appropriately scaled parameters. We assume that the theorem applies to the present case, and thereby obtain the final result for $\Phi_M(t)$,

$$\Phi_M(t)=\frac{1+2\cos\Omega_0' t}{3}\exp(-t/\tau_R')$$

$$\times[1-\langle\gamma'^2\rangle+\langle\gamma'^2\rangle\cos(\omega_0' t)\exp(-t/\tau_V')], \quad (15)$$

where the "primed" parameters will in general be different from the corresponding "unprimed" variables in the self-correlation function.

The dielectric spectrum arising from Eq. (15) can be obtained using the linear-response relation valid for the conducting boundary conditions used in our simulations,[15]

$$\frac{\epsilon(\omega)-1}{\epsilon(0)-1}=1+i\omega\Phi_M(\omega), \quad (16)$$

where $\Phi_M(\omega)$ is the Fourier transform of $\Phi_M(t)$. Note that different boundary conditions would give rise to different $\Phi_M(t)$ [i.e., different parameters in Eq. (15)], but the same dielectric spectrum would result. The expression for $\Phi_M(\omega)$ is somewhat messy, but by noting that the characteristic frequencies and relaxation times for chain and single-particle motion are very different ($\omega_0 \gg \Omega_0$, $\tau_R \gg \tau_V$), the following approximations to the real and imaginary parts of $\Phi_M(\omega)$ can be obtained:

TABLE I. Parameters obtained by "fitting" the simple theoretical model.

Method	ρ^*	$\tau_R'^*$	$\tau_V'^*$	$\langle\gamma'^2\rangle$	$\omega_0'^*$
MD	0.06	65	0.35	0.006	47
	0.17	41	0.27	0.006	45
	0.35	24	0.18	0.006	40
BD	0.06	890	0.11	0.008	45
	0.17	480	0.10	0.008	42
	0.35	110	0.10	0.008	36

$$\Re\Phi_M(\omega)=\frac{1-\langle\gamma'^2\rangle}{3}\left[\frac{\tau_R'}{1+\omega^2\tau_R'^2}+\frac{\tau_R'}{1+(\omega+\Omega_0')^2\tau_R'^2}\right.$$

$$\left.+\frac{\tau_R'}{1+(\omega-\Omega_0')^2\tau_R'^2}\right]+\frac{\langle\gamma'^2\rangle}{2}$$

$$\times\left[\frac{\tau_V'}{1+(\omega+\omega_0')^2\tau_V'^2}+\frac{\tau_V'}{1+(\omega-\omega_0')^2\tau_V'^2}\right], \quad (17)$$

$$\Im\Phi_M(\omega)=\frac{1-\langle\gamma'^2\rangle}{3}\left[\frac{\omega\tau_R'^2}{1+\omega^2\tau_R'^2}+\frac{(\omega+\Omega_0')\tau_R'^2}{1+(\omega+\Omega_0')^2\tau_R'^2}\right.$$

$$\left.+\frac{(\omega-\Omega_0')\tau_R'^2}{1+(\omega-\Omega_0')^2\tau_R'^2}\right]+\frac{\langle\gamma'^2\rangle}{2}$$

$$\times\left[\frac{(\omega+\omega_0')\tau_V'^2}{1+(\omega+\omega_0')^2\tau_V'^2}+\frac{(\omega-\omega_0')\tau_V'^2}{1+(\omega-\omega_0')^2\tau_V'^2}\right]. \quad (18)$$

IV. RESULTS AND DISCUSSION

As noted above, we have carried out both MD and BD simulations. For ferrofluid suspensions the BD calculations

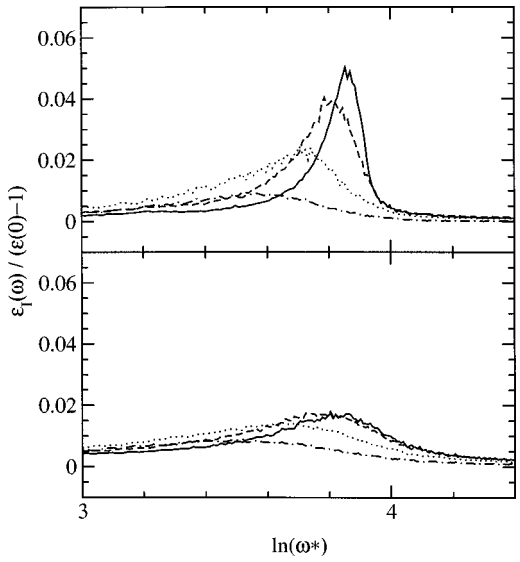

FIG. 1. The imaginary parts of $\epsilon(\omega)$ for different densities. The upper curves are MD results and the lower are BD results obtained with $\Theta^*=4$ and $D^*=0.04$. The solid, dashed, dotted, and dotted-dashed curves are for $\rho^*=0.06$, 0.17, 0.35 and 0.5, respectively.

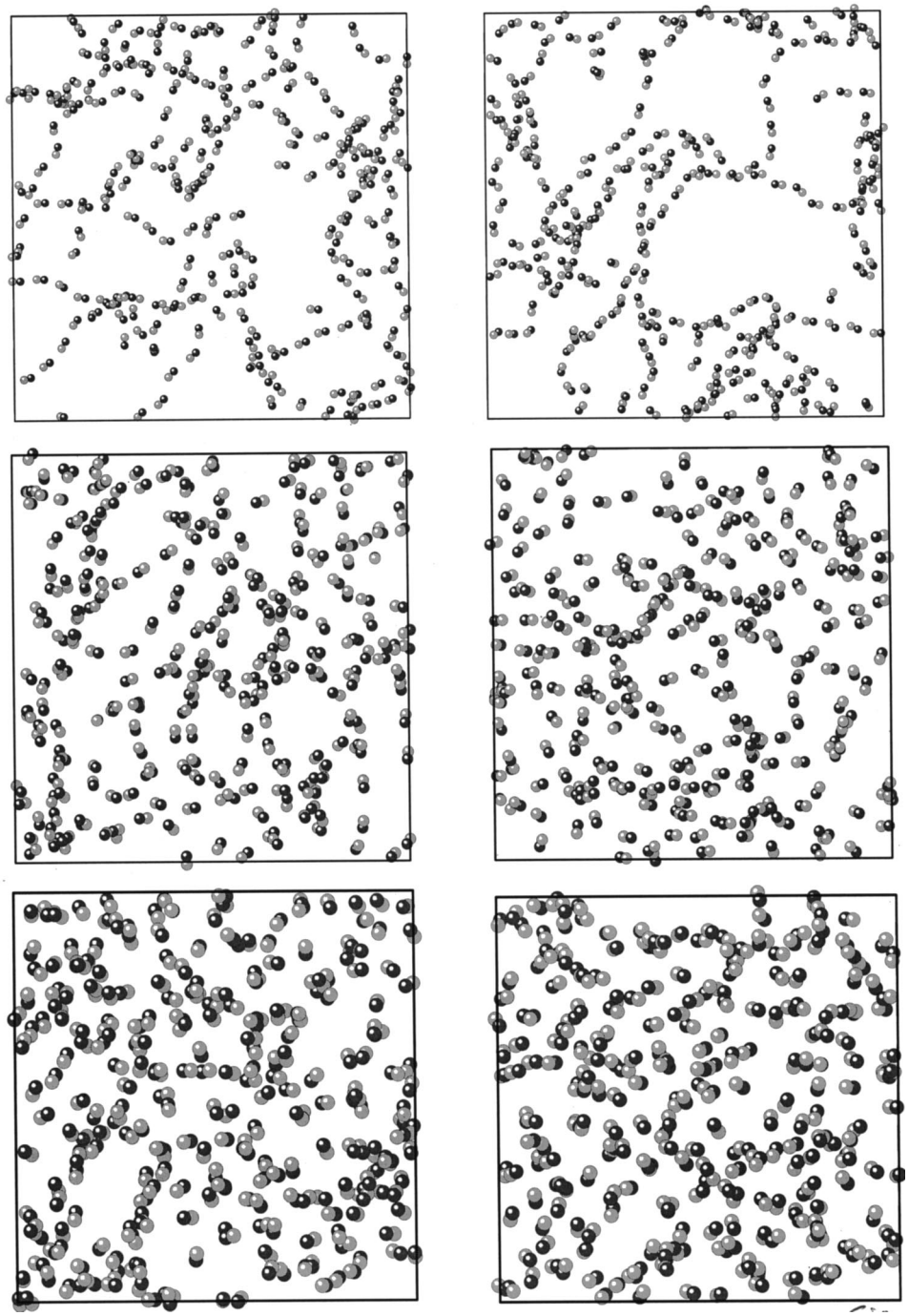

FIG. 2. The variation of the dipolar fluid structure with density for BD (left) and MD (right) calculations. The diffusion constants are as in Fig. 1. The dipolar particles are depicted as ''dumbbells'' with the positive and negative ends of the dipoles indicated by light and dark spheres. Note that the particles appear larger at higher density because the ratio L/σ is smaller. The particle center-of-mass coordinates are projected onto a plane parallel to a side of the simulation cell. The results shown are for $\rho^*=0.06$ (top), 0.17 (middle), and 0.35 (bottom).

are likely the more realistic, but the MD method provides a useful comparison and we begin with a brief discussion of these results.

All MD calculations were carried out at $T^*=1.35$, $\mu^*=3.0$ and $I^*=0.025$, and the temperature was constrained using a Gaussian isokinetic thermostat.[7,16,17] Results were obtained for the three densities $\rho^*=0.06$, 0.17, and 0.35, which roughly correspond to the three ''phases'' identified in earlier work.[4] Also, for comparison purposes, calculations were carried out at the higher density $\rho^*=0.5$, where the dipolar fluid behaves as a ''normal'' isotropic liquid with little or no tendency to form distinct long-lived chains. For the three lowest densities two well-separated relaxation channels were observed that, following the above discussion, we associate with chain rotation (τ_R) and with dipolar vibration within chains (τ_V). Estimated values of the relaxation times and other parameters obtained by ''fitting'' Eq. (15), or Eqs. (17) and (18), are given in Table I. The simulation runs were not sufficiently long to determine the very low frequency behavior accurately, and hence reliable estimates of Ω_0' were not obtained.

We note that, as one would expect, $\tau_V'^*$ is much smaller than $\tau_R'^*$. The high frequency behavior of $\epsilon_I(\omega)$ is most interesting and is plotted in Fig. 1. The band at $\omega^*\simeq 45$ is due to the vibrational motion of dipoles within chains, and is a signature of chain formation. This feature of the dielectric spectrum (or rather the frequency-dependent magnetic sus-

ceptibility) could be used to study chain formation in colloidal ferrofluids. As we would expect, the peak is sharpest and best resolved at the lower densities where the chains are most distinct and independent (see snapshots[18] in Fig. 2). As the density is decreased, the peak moves to lower frequencies and broadens, finally becoming very weak at $\rho^*=0.5$, where the dipolar system behaves as a ''normal'' fluid characterized by single particle diffusion, and distinct long-lived chains are no longer a significant factor.

It is of interest to examine chain formation at very low densities (e.g., $\rho^*=0.001$), but converged MD results were not possible in this regime. At low densities there are not enough interparticle collisions to achieve equilibrium, and the dipoles simply ''freeze'' into assorted chains that rotate such as to maintain the total rotational kinetic energy dictated by the thermostat. The ''final'' structures are highly dependent on the initial conditions and true equilibrium is not achieved. Hence, we were motivated to employ BD which allows for more realistic thermal motion by introducing random forces and torques resulting from collisions with ''solvent'' particles.

At intermediate and high densities BD simulations were carried out with $\Theta^*=4.0$ and $D^*=0.04$. These diffusion coefficients were estimated from velocity autocorrelation functions obtained in MD simulations, and it can be seen from Fig. 2 that at the intermediate densities the BD chaining patterns are very similar to those obtained in the MD calculations. The dielectric spectra are qualitatively similar to the MD results in that two distinct relaxation channels are observed. However, the high frequency vibrational bands in $\epsilon_I(\omega)$ are considerably broader than in the MD case. The broadening of the vibrational bands is easily understood since we would expect the random torques to give rise to somewhat looser chains, and hence increase the motion of individual dipoles. Nevertheless, it is clear that for reduced densities in the range 0.06 to 0.5, the MD and BD simulations give the same physical picture and qualitatively similar dielectric spectra.

We have also carried out BD calculations at $\rho^*=0.001$ for different values of Θ^* and D^*, which lead to different steady-state temperatures and to different structures, as shown in Fig. 3. We note that the dipolar association into chains and rings increases as we increase Θ^* and D^* (i.e., decrease the solvent viscosity). Corresponding $\epsilon_I(\omega)$ results are plotted in Fig. 4. We see that $\epsilon_I(\omega)$ varies quite substantially as the diffusion constants are increased. At the lowest values there is a single broad band peaked at $\ln(\omega^*)\simeq 2$. This is close to the value we would expect for free rotors [$\omega=\sqrt{2kT/I}$, $\ln(\omega^*)=2.34$ at $T^*=1.35$], and is consistent with the fact that the snapshot (Fig. 3) shows little association for these parameters. At the intermediate diffusion constants $\epsilon_I(\omega)$ displays considerably more structure; the ''free rotor'' band is still present, but a very broad band now appears at lower frequency and small peaks occur at higher frequencies. In light of the structure evident in Fig. 3, we associate the low-frequency band with the rotation of chains of varying length, and the high-frequency bands with the vibration of chained dipoles. The highest frequency peak likely arises from dipoles within chains, and the small peak at somewhat lower frequency is possibly due to ''terminal'' dipoles that are bound to other dipoles only at one end (there are quite a lot of these in this system). At the largest diffusion constants, the free rotor band is very weak and strong bands are present

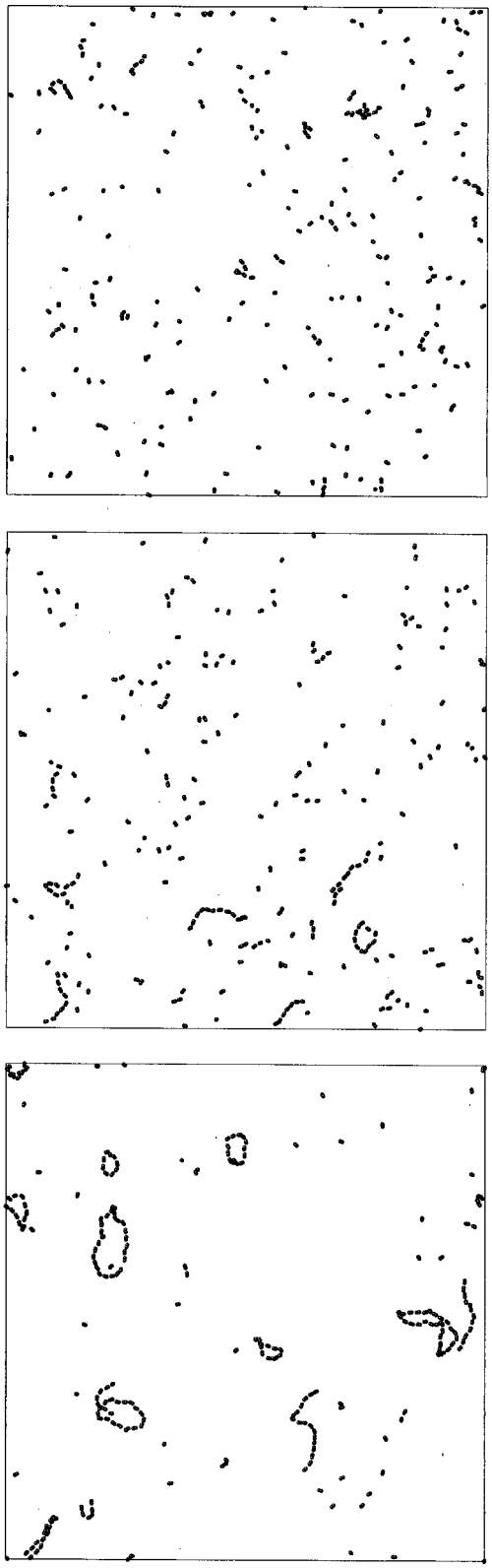

FIG. 3. The structure of a low density ($\rho^*=0.001$) dipolar fluid modeled using BD with different parameters describing the coupling to the ''solvent bath.'' Results are shown for the following parameters: (top) $\Theta^*=4$, $D^*=0.04$; (middle) $\Theta^*=400$, $D^*=4.0$; (bottom) $\Theta^*=4000$, $D^*=40$.

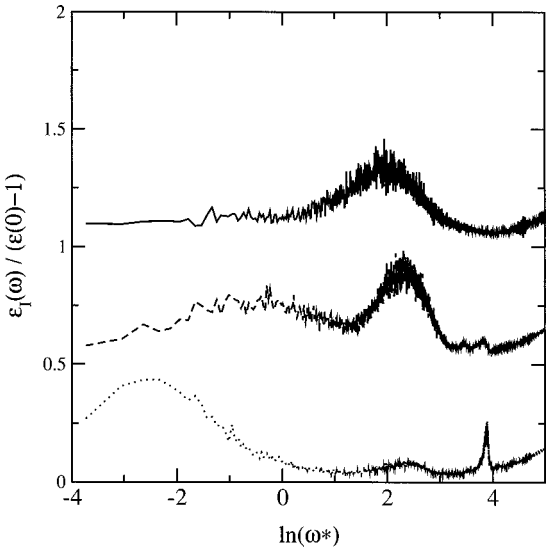

FIG. 4. BD results for the imaginary part of $\epsilon(\omega)$ for a dipolar fluid at $\rho^*=0.001$. The curves shown are for: (top) $\Theta^*=4$, $D^*=0.04$; (middle) $\Theta^*=400$, $D^*=4.0$; (bottom) $\Theta^*=4000$, $D^*=40$. Note that for clarity the middle and top curves have been shifted upward by 1 and 2 units, respectively.

at both low and high frequency. In this system most particles are associated into rather long chains; hence, the low-frequency band is due to the relaxation of associated species, and the sharp, high-frequency peak is due to the vibrational motion discussed previously.

It interesting to further examine the simple theory described above by making more direct comparisons with the BD simulation results. To this end, the real parts of $\Phi_S(\omega)$ and $\Phi_M(\omega)$ are plotted in Fig. 5. The theory predicts that $\omega_0^*=41$ and $\langle\gamma^2\rangle=0.0645$ (see Ref. 11). These values together with $\tau_V^*=0.1$ (see Table I) give the dotted curve in Fig. 5. We see that the theoretical frequency is somewhat high, and that better agreement is obtained with $\omega_0^*=30$; nevertheless, the simple theory clearly provides at least a rough description of the vibrational motion. The real part of $\Phi_M(\omega)$ also has a peak in the same frequency region, but is much less intense. Further, as we would expect from the discussion in Sec. III, the parameters required to "fit" this curve differ from those given by the simple theory for the self-correlation function (note in particular that $\langle\gamma'^2\rangle$ is much smaller than $\langle\gamma^2\rangle$).

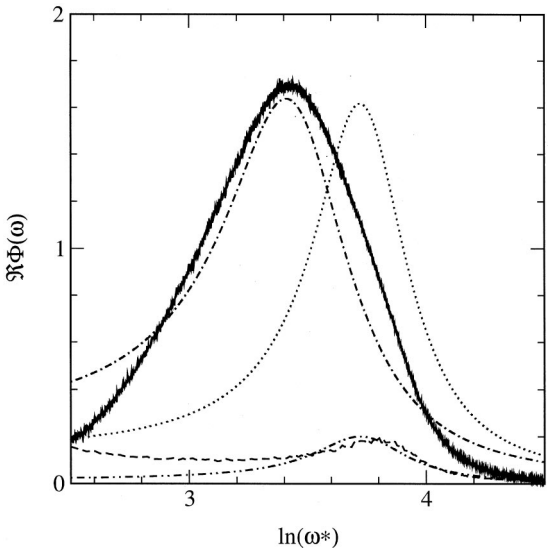

FIG. 5. Comparison of theory and BD simulation results ($\rho^*=0.06$, $D^*=0.04$, $\Theta^*=4$) for the real parts of $\Phi_S(\omega)$ and $\Phi_M(\omega)$. The solid and dashed curves are BD results for $\Re\Phi_S(\omega)$ and $\Re\Phi_M(\omega)$, respectively. The remaining curves represent the following model calculations: dotted, $\tau_V^*=0.1$, $\langle\gamma^2\rangle=0.0645$, $\omega_0^*=41$; dashed-dotted, $\tau_V^*=0.1$, $\langle\gamma^2\rangle=0.0645$, $\omega_0^*=30$; dashed-dotted-dotted, $\tau_V'^*=0.1$, $\langle\gamma'^2\rangle=0.008$, $\omega_0'^*=45$.

V. SUMMARY AND CONCLUSIONS

In this paper we have closely examined the dielectric spectra of strongly interacting dipolar fluids. Our main purpose was to identify features that relate to dipolar association (chaining) in colloidal ferrofluids at low temperatures and densities. We have carried out both molecular and Brownian dynamics simulations for several densities characteristic of the different phases previously identified for dipolar fluids. Although there are differences in detail, qualitatively, both simulation methods give similar results, except at very low densities where the MD calculations do not converge in reasonable simulation times. Our main observation is the presence of a high-frequency band clearly associated with the vibrational motion of particles *within* dipolar chains. This feature is significant only at densities (and temperatures) sufficiently low that long-lived dipolar chains are present; it disappears as the chains break up with increasing density, and is not a feature of "normal" dipolar fluids characterized by single particle diffusion. This high-frequency band should prove useful in the study of chain formation in strongly interacting ferrofluids, and could possibly help in the experimental elucidation of their rather complex and unusual phase behavior.[4,6]

In addition to the simulations, we have presented a simple theory that provides analytical expressions for the dielectric function of associated dipolar fluids. The theory relates the interesting high-frequency band to the strength of the dipolar interaction, and predicts characteristic vibrational frequencies as well as other parameters. Comparisons with simulation results indicate that, while the theory is somewhat rough quantitatively, it does give a good qualitative description of the high-frequency relaxation.

ACKNOWLEDGMENTS

The financial support of the National Science and Engineering Research Council of Canada is gratefully acknowledged. One of the authors (V.V.M.) would like to thank the Killam Foundation for financial support.

[1] T. Tlusty and S. A. Safran, Science **290**, 1328 (2000), and references therein.
[2] P. J. Camp and G. N. Patey, Phys. Rev. E **62**, 5403 (2000), and references therein.
[3] D. Wei and G. N. Patey, Phys. Rev. Lett. **68**, 2043 (1992); Phys. Rev. A **46**, 7783 (1992).
[4] P. J. Camp, J. C. Shelley, and G. N. Patey, Phys. Rev. Lett. **84**, 115 (2000).
[5] P. H. Hess and P. H. Parker, Jr., J. Appl. Polym. Sci. **10**, 1915 (1966).
[6] H. Mamiya, I. Nakatani, and T. Furubayashi, Phys. Rev. Lett. **84**, 6106 (2000).

[7] M. P. Allen and D. J. Tildesley, *Computer Simulation of Liquids* (Clarendon, Oxford, 1987).
[8] W. F. van Gunsteren and H. J. C. Berendsen, Mol. Phys. **45**, 637 (1982).
[9] A. Papazyan and M. Maroncelli, J. Chem. Phys. **102**, 2888 (1995).
[10] S. W. De Leeuw, J. W. Perram, and E. R. Smith, Proc. R. Soc. London, Ser. A **373**, 27 (1980); **373**, 57 (1980).
[11] Of course the chains are not of infinite length, but our estimates are not very sensitive to this assumption. For example, if we take the other extreme and consider only nearest-neighbor interactions, the quantity $\zeta(3) = 1.202$ in Eq. (2) is replaced by unity. The estimated vibrational frequency, ω_0^*, then becomes 37 rather than 41, and the mean square polar angle between a dipole and the local chain direction, $\langle \gamma^2 \rangle$, changes from 0.064 to 0.078.
[12] T. Keyes and D. Kivelson, J. Chem. Phys. **56**, 1057 (1972).
[13] D. Kivelson and P. A. Madden, Mol. Phys. **30**, 1749 (1975).
[14] H. Goldstein, *Classical Mechanics*, 2nd ed. (Addison-Wesley, London, 1980).
[15] P. Madden and D. Kivelson, Adv. Chem. Phys. **56**, 467 (1984).
[16] D. J. Evans and G. P. Morris, *Statistical Mechanics of Nonequilibrium Liquids* (Academic, London, 1990).
[17] G. P. Morris and C. P. Dettmann, Chaos **8**, 321 (1998).
[18] Extensive aggregation and chaining at the lowest density is obvious from the snapshots shown in Fig. 2, but the fact that chaining becomes much less important at the higher densities might not be evident from these two-dimensional projections. However, the detailed analysis of the static structure factors given in Ref. 2 shows that this is indeed the case.